

Flux tube disconnection - An example of 3D reconnection

A.L. Wilmot-Smith, E.R. Priest

School of Mathematics and Statistics, University of St Andrews,

North Haugh, St Andrews, Fife, KY16 9SS, UK

August 15, 2007

Abstract

Magnetic reconnection in three-dimensions (3D) is fundamentally different in many respects from its two-dimensional counterpart. An analytical example of a global 3D general magnetic reconnection process is presented here, in which a magnetic flux tube has its footpoints rotated in different directions. A localised non-ideal region is found in the centre of the tube where the field lines are twisted as a result of the footpoint counter-rotation. A qualitative analysis demonstrates how the parameters that determine the strength and geometry of the magnetic field depend on the rotational driving velocity. The reconnection rate measures the rate at which field lines within the entire flux tube are changing their magnetic connections, and is shown to be proportional to the driving velocity imposed on its footpoints. The qualitative estimates are confirmed by an exact kinematic 3D magnetohydrodynamic analytical solution, which possesses a localised three-dimensional current and determines the reconnection rate quantitatively.

I Introduction

Magnetic reconnection is a fundamental process that is responsible for a wide range of dynamic events in astrophysical, space and laboratory plasmas. Reconnection allows for a change in topology of an otherwise ideal plasma and can result in substantial energy release – it was first suggested as a mechanism for particle acceleration in solar flares [1].

The first models for reconnection were two-dimensional (2D) (i.e. the flow and field are confined to the (x, y) plane and $\partial/\partial z = 0$). Under these circumstances reconnection can only occur at an X-type null-point of the field, with the rate at which it occurs being given by the electric field at the X-point and measuring the amount of flux being cut and rejoined. In 2D models, magnetic flux is transported by a plasma flow toward the null-point, where it is reconnected and, subsequently, transported away from the null-point at a relatively high speed.

In the first quantitative model for the process, the Sweet-Parker model [2, 3], a current sheet with length equal to the global length-scale is contained within oppositely directed magnetic fields. The reconnection rate is proportional to $S^{-1/2}$ (where S is the Lundquist number) and, so, with the high values of S in space and astrophysical plasmas, it is too slow to account for observed events such as solar flares. To overcome this problem, the Petschek model [4] takes a much shorter current sheet with a standing slow shock at each of its corners and achieves a reconnection rate dependent on $1/\ln S$. In both the Sweet-Parker and Petschek models, magnetic energy is converted to thermal energy via Ohmic heating and also to kinetic energy of the plasma, with most of the conversion in the Petschek process taking place at the standing shocks.

Reconnection models that scale as the Sweet-Parker rate (or slower) are described as *slow* whilst those that scale faster than $S^{-1/2}$ (including the Petschek model) are described as *fast* [5]. We now understand that the Petschek model is just one of a much wider class of fast reconnection solutions that includes families of *almost-uniform* [6] and *non-uniform* [7] regimes; which solution is achieved in numerical simulations depends on the boundary conditions imposed

[8]. Petschek reconnection itself appears to also require a nonuniform localised resistivity to be imposed [9, 10]. However, localised regions of enhanced resistivity are expected to occur in practice (since intense current concentrations are likely to drive microinstabilities that themselves enhance the resistivity) and so this requirement is not thought to be unreasonable. Reconnection may also arise as a result of an initial localised instability, such as the tearing mode [11] and in these situations the dynamics are not so sensitive to the choice of boundary conditions. Local plasma conditions, such as the presence of an anomalous resistivity, may also play an important role in determining the resulting reconnection configuration [12]. For a review of 2D reconnection see, for example, Ref. [5].

Moving into 2.5D and 3D configurations, reconnection events that exhibit several similarities to the 2D case have been modelled. For example, Ugai and Zheng [13] found a 3D fast reconnection configuration including standing slow shocks to be set up when a small disturbance together with an enhanced resistivity was imposed on a current sheet. A 3D configuration with Petschek-like properties, including slow shocks, was also obtained by Linton and Longcope [14] after they imposed a short burst of reconnection in a localised sphere. Several 3D effects were also observed in this case, with the shock-geometry being substantially modified. In a 2.5D study of the interaction of two emerging flux systems, Archontis *et al.* [15] found Petschek-like reconnection with slow-mode shocks extending from the current sheet that formed at the interface between the two flux systems. The nature of the reconnection remained the same for both uniform and non-uniform examples of resistivity.

However, not all 3D reconnection configurations show similarities to the 2D case and three-dimensional field configurations result in a much wider class of reconnection solutions. Indeed, while several features of 2D reconnection models, such as a plasma flow across the separatrices of the field, or a normal electric field component at the X-point, were proposed as definitions for reconnection, it was not until more general, 3D, circumstances were considered that the appropriateness of each of these conditions became clear. In Ref. [16] the applicability

of these ideas to 3D geometries was considered. The authors argued that any general definition should be structurally stable, i.e. not depend on small modifications to the system under consideration. They proposed that a definition, first considered by Ref. [17], based on a change of connectivity of plasma elements due to a localised violation of the frozen-in field condition should be used. This forms the basis of *General Magnetic Reconnection* (GMR). The condition

$$\int E_{\parallel} dl \neq 0,$$

evaluated along a field-line, is required for GMR, being a generalisation to 3D of the 2D normal electric field component at an X-point. In order to distinguish between reconnection and diffusive processes, the additional requirement that the non-ideal term in Ohm's law (which itself is the cause of the breakdown of the frozen-in condition) be localised is also imposed. Equivalently, GMR applies only to situations where global magnetic Reynolds number (R_{me}) is large, i.e. $R_{me} \gg 1$. Figure 1 illustrates the regimes of breakdown of magnetic connection and so also the branches of general magnetic reconnection ([16]). The breakdown of magnetic connection may be caused by a resistive term in Ohm's law, but also by other non-ideal terms, such as the pressure tensor.

In 3D, there are several forms of reconnection associated with magnetic null-points. Magnetic *separators*, field lines connecting two null-points and so lying at the interface between four distinct flux-domains, are thought to be favourable locations for current build-up ([18], [19]). Separator reconnection occurs along separators connecting null-points ([20, 21, 22]) and has been observed in many numerical experiments (e.g. [23, 24, 25, 26]). Reconnection may also be linked to the *spine* and *fan* associated with null-points, depending on the direction of the current ([27, 28]).

Finite-B reconnection assumes the magnetic field does not vanish within the non-ideal region, and may be classified further as *local* or *global* according to how the change in connectivity arises. If a change in magnetic connectivity occurs for plasma elements that do not themselves pass through the non-ideal region then the process is global; otherwise it is local. The change in connectivity necessarily involves plasma elements located on different sides of the non-ideal region, and

reconnection occurs only for elements which are, at some time, connected to the non-ideal region.

The complexity of 3D reconnection has meant that much of the analytical work so far has focused on the *kinematic* problem, where the implications of the momentum equation are ignored and the effects of Ohm's law, together with Maxwell's equations and the continuity equation are considered ([29] and other references). In these studies a particular magnetic field configuration is imposed from which the plasma velocity and electric field is deduced. The simplified nature of the analysis allows an isolated non-ideal region to be taken (i.e. bounded in all three dimensions). Such a localised non-ideal region is the generic situation in astrophysical plasmas. The models have identified several new features of 3D reconnection. For example, under certain circumstances, reconnection solutions may be decomposed into ideal and non-ideal parts according to

$$\mathbf{E}_{non-id} + \mathbf{v}_{non-id} \times \mathbf{B} = \frac{1}{\sigma} \mathbf{j},$$

$$\mathbf{E}_{id} + \mathbf{v}_{id} \times \mathbf{B} = \mathbf{0},$$

i.e. there is no longer a direct coupling between particular non-ideal reconnective solutions and ideal flows. The localisation of the non-ideal region implies the existence of counter-rotating plasma flows within the flux-tube that consists of all the field lines threading the non-ideal region. Both of these new features have subsequently been backed up by dynamic analytical modelling ([30]) as well as by 3D MHD simulations ([31]).

Reconnection models in which the magnetic field has an O-type topology have received little attention thus far. Recently, however, Ref. [32] presented numerical simulations of 3D reconnection due to rotational motion of the footpoints of magnetic flux tubes. In their simulations stagnation flows were observed, together with an X-type current structure, although the magnetic field showed an O-type configuration in cross-sectional planes. Here we present an example of 3D reconnection in an elliptic geometry which allows for analytical modelling, namely the reconnection that occurs as a result of the counter-rotation of the ends of a magnetic flux tube, which we refer to as *flux-tube disconnection*. A

qualitative description of the process is outlined in the next section, where we also demonstrate how it fits into the theme of GMR but looks very different from previously considered reconnection models. A more detailed quantitative description is given in Sec. III.

II A qualitative model for flux-tube disconnection

Consider a steady-state situation (Figure. 2) where a magnetic flux tube, of radius a , has footpoints located at $z = \pm H$ and a typical vertical magnetic field strength b_0 . Assume that the two footpoint ends are being rotated in different directions with speed v_0 , and that, as a result of the counter-rotation, a twist in the field is produced within $z = \pm L$. That is, assume that within the non-ideal region the magnetic field may be written as

$$\mathbf{B} = B_\theta \hat{\theta} + B_z \hat{z}, \approx kb_0 \hat{\theta} + b_0 \hat{z},$$

where k is a constant indicating the order of magnitude ratio of the toroidal field strength to the guide field. The flow is assumed to be incompressible, which is satisfied automatically for a purely azimuthal plasma velocity that is independent of θ .

The localised poloidal field component results in a current, and therefore a non-ideal region, that is localised in all three dimensions. The current has a component parallel to the magnetic field, and does not close within the non-ideal region; we assume that the return current is diffuse and is spread over a sufficiently large volume that its local effect may be neglected. A sketch of the current structure is shown in Figure. 3.

Several questions now arise in the analysis. How, in an order of magnitude sense, is the twist in magnetic field related to the driving plasma velocity v_0 . Specifically, how do the parameters L and k , which determine the extent of the non-ideal region and the strength of the poloidal field, respectively, depend on v_0 ? Which parameters determine the rate of reconnection? How is the rate of

reconnection dependent on the driving velocity v_0 ?

We can gain an insight into these questions by examining Ohm's law and Faraday's law for a steady state:

$$\mathbf{E} + \mathbf{v} \times \mathbf{B} = \frac{1}{\sigma} \mathbf{j},$$

$$\nabla \times \mathbf{E} = \mathbf{0},$$

where σ is the electrical conductivity. Consider the ideal region above and below $z = \pm L$. There $\mathbf{j} = 0$, and Ohm's law reduces to

$$E_r + v_0 b_0 = 0, \quad (1)$$

where E_r is the typical radial electric field. Similarly, along the central axis ($r = 0$) the plasma velocity is zero by symmetry and

$$E_z = \frac{1}{\sigma} j_z. \quad (2)$$

Now, $\nabla \times \mathbf{B} = \mu \mathbf{j}$ implies that along the axis we also have

$$j_z = \frac{1}{\mu} \left(\frac{B_\theta}{r} + \frac{\partial B_\theta}{\partial r} \right) \approx \frac{2kb_0}{\mu a}. \quad (3)$$

Next consider a loop integral, as illustrated in Figure 4, consisting of the part of the central field line from below to above the non-ideal region, a field line on the boundary of the non-ideal region, and two connecting radial lines. Integrating around this loop and using Faraday's law and using the symmetry of solutions above and below the z -axis gives

$$0 = \oint \mathbf{E} \cdot d\mathbf{l} \approx 2LE_z + 2aE_r, \quad (4)$$

since the electric field along the boundary of the non-ideal region vanishes. Substituting expressions (1), (2) and (3) into relation (4) allows us to eliminate the electric fields E_r and E_z and obtain an expression for the plasma velocity in terms of the field parameters:

$$v_0 = \frac{2\eta kL}{a^2}, \quad (5)$$

where $\eta = 1/\sigma\mu$ is the magnetic diffusivity. This expression allows us to determine the product kL when the radius of the tube (a) and the rotational driving

velocity (v_0) are given. For example, if we keep the height of the non-ideal region (L) fixed, any increase in v_0 must be reflected by an increase in the poloidal field strength (k) i.e., the number of turns the field makes within the non-ideal region must increase. Similarly, we could have kept k fixed but increased L ; this would also have the effect of increasing the number of turns the field makes within the non-ideal region. Therefore we deduce that the effect of an increase in rotation speed (v_0) is to increase the number of turns of the field, whether through a lengthening of the non-ideal region or by an increase in the number of turns of the field within the non-ideal region.

Equation (5) is the basic expression for the rotational velocity (v_0) in terms of the magnetic diffusivity (η), the dimensions (a, L) of the diffusion region and the ratio (k) of rotational to axial field strength. It is interesting to see how it differs from the corresponding simple expression ($v_0 = \eta/a$) for the inflow into a Sweet-Parker diffusion region, since here we have the extra factors k and L/a that arise from the three-dimensionality of our process. The first factor arises essentially because we have a twisting process and the second because the electric field components E_z and E_r differ in magnitude.

We may also make an estimate of the rate of reconnection ($d\Phi_{rec}/dt$), i.e. the rate of change of magnetic flux. This rate is given by the integral of the parallel electric field along the reconnection line, i.e. along the central axis:

$$\frac{d\Phi_{rec}}{dt} = \int E_{\parallel} dl \approx 2LE_z \approx \frac{4\eta kb_0 L}{a} = 2b_0 a v_0, \quad (6)$$

where the above expressions, (1), (2) and (3), have been used. This shows us that the rate of reconnection is proportional to the rotational driving velocity. The reconnection rate may be interpreted as the rate at which all the field lines within the flux tube are changing their connections, and so this estimate of the reconnection rate agrees with our intuitive understanding of the process. In dimensionless terms we have

$$\frac{d\bar{\Phi}_{rec}}{dt} = 2 \frac{a}{H} \frac{v_0}{v_A}. \quad (7)$$

Thus the dimensionless reconnection rate is proportional to the Alfvén Mach number (v_0/v_A) of the driving flow and the ratio (a/H) of the non-ideal region

radius (a) to the ambient scale height (H). Thus, if a/H and v_0/v_A are significant fractions of unity we have fast reconnection, i.e., at a significant fraction of the Alfvén speed; otherwise the reconnection is slow (see Sec. IV).

In the next section we present an analytical model for the reconnection process described above. We show that the exact kinematic solution obtained there agrees with the intuitive understanding developed in this section.

III Kinematic model

We present here an axisymmetric analytical model for flux tube disconnection. The model is kinematic (i.e. the equation of motion is neglected) and stationary, and satisfies the following equations:

$$\mathbf{E} + \mathbf{v} \times \mathbf{B} = \frac{1}{\sigma} \mathbf{j}, \quad (8)$$

$$\nabla \times \mathbf{E} = \mathbf{0}, \quad (9)$$

$$\nabla \times \mathbf{B} = \mu \mathbf{j},$$

$$\nabla \cdot \mathbf{B} = 0,$$

$$\nabla \cdot \mathbf{v} = 0.$$

Several of the previous 3D analytical models of reconnection which have helped to increase our understanding of the process have been kinematic ([33, 29, 28]). Neglecting the momentum equation allows for analytical progress to be made and, as a result, several new features of 3D reconnection have been found, such as counter-rotational plasma flows, that are not present in 2D. The features are expected to be inherent to the 3D reconnection processes, and not consequences of considering only a subset of the MHD equations. Indeed, using kinematic models as a guide, subsequent numerical experiments (such as that of Ref. [31]) and analytical models with the momentum equation included ([30]) have investigated the suggested features and confirmed their importance in the 3D process.

A typical feature of reconnection in astrophysical plasmas is that non-ideal regions are localised in 3D as a result of intense current concentration. In such

regions the resistivity is expected to be enhanced by current-driven microinstabilities. We therefore consider here a magnetic field that leads to a localised current, and additionally impose a localisation of the resistivity. This is one of the features that distinguishes our model from previous kinematic models where a localised non-ideal region was obtained through an enhancement of the resistivity alone.

Working throughout in cylindrical coordinates (r, θ, z) , the magnetic field is prescribed as

$$\mathbf{B} = 2b_0k\frac{r}{a} \exp\left(-\frac{r^2}{a^2} - \frac{z^2}{L^2}\right) \hat{\theta} + b_0\hat{z}.$$

The azimuthal component of the magnetic field is localised and so generates a twist in the magnetic field close to the origin, while at large distances the field is uniform in the z -direction. The width of the flux tube is dependent on the parameter a , the extent of the twist in the z -direction on the parameter L , and the ratio of the toroidal field to the guide (or axial) field given by the parameter k . Some typical field lines are illustrated in Figure 5; note that each field line remains on a surface of constant radius.

This simple field configuration allows for a direct integration to find the equations of the field lines. This proves to be useful later, where we integrate along the field lines in order to obtain expressions for the remaining terms. The equations, $\mathbf{R}(r_0, \theta_0, s)$ of the field lines passing through the point $(r_0, \theta_0, z = 0)$ are given by

$$\begin{aligned} R &= r_0, \\ \Theta &= 2b_0k\frac{r_0}{a} s \exp\left(-\frac{r_0^2}{a^2} - \frac{b_0^2s^2}{L^2}\right), \\ Z &= b_0s. \end{aligned} \tag{10}$$

The inverse mapping, $\mathbf{R}_0(r, \theta, s)$, is given by

$$\begin{aligned} R_0 &= r, \\ \Theta_0 &= 2kb_0s\frac{r}{a} \exp\left(-\frac{r^2}{a^2} - \frac{b_0^2s^2}{L^2}\right), \\ Z_0 &= -b_0s. \end{aligned} \tag{11}$$

The twist of the flux tube generates closed poloidal rings of current, given

by

$$\mathbf{j} = \frac{4b_0k}{\mu a} \exp\left(-\frac{r^2}{a^2} - \frac{z^2}{L^2}\right) \left(\frac{rz}{L^2}\hat{\mathbf{r}} + \frac{a^2 - r^2}{a^2}\hat{\mathbf{z}}\right).$$

An example is shown in Figure 6, where the current is seen to be localised in three-dimensions around the origin, and has its greatest strength along the axis of the flux tube. Now the non-ideal term, $\frac{1}{\sigma}\mathbf{j}$ in Ohm's law (8) would already be localised given a uniform electrical conductivity, σ . Here, however, we choose to impose in addition a form for $1/\sigma$ leading to a localised magnetic diffusivity η . We take

$$\eta = \frac{1}{\sigma_0\mu} \exp\left(-\frac{4r^2}{a^2} - \frac{z^2}{L^2}\right). \quad (12)$$

Regions of intense current concentration are expected to give rise to enhanced diffusivity due to current-driven microinstabilities. This consideration provides a motivation for the form of η chosen here, which encompasses the location of strongest current. We define the non-ideal region, D , to be inside the surface defined by $|\mathbf{j}|/\sigma = 0.02 (|\mathbf{j}|/\sigma)_{\max}$. The exact profile of η , given by equation (12) has been chosen to ensure there is no return-current within D . This is expected to be the case if the rotational plasma flows at the tube footpoints possess a single sign in planes of constant z . With the localisation imposed on η , the results presented here are qualitatively the same as in a model in which the return current is very diffuse. However, a similar analysis to that presented here may be carried out with $\eta = \eta_0 = \text{constant}$. The results (given in Appendix A) also represent an example of flux-tube disconnection with qualitatively similar properties to that outlined here.

Combining (8) and (9) and taking $\mathbf{E} = -\nabla\phi$ gives

$$-\nabla\phi + \mathbf{v} \times \mathbf{B} = \frac{1}{\sigma}\mathbf{j}. \quad (13)$$

The non-ideal term $\eta\mathbf{j}$ is now known, and we are left to deduce ϕ and \mathbf{v} . The component of (13) parallel to the magnetic field is given by

$$-\nabla\phi \cdot \mathbf{B} = \frac{1}{\sigma}\mathbf{j} \cdot \mathbf{B}$$

and so an expression for ϕ can be found by integrating along the magnetic field lines, expressions for which are given by (10). Starting the integration from the

initial condition $\phi = \phi_0(r_0, \theta_0)$ at $z = 0$ we deduce that

$$\phi(r_0, \theta_0, s) = - \int_0^s \frac{1}{\sigma} \mathbf{j} \cdot \mathbf{B} ds + \phi_0(r_0, \theta_0). \quad (14)$$

An equivalent expression for ϕ in terms of (r, θ, z) can then be obtained using the inverse field line mappings given by (11).

The initial integration condition $\phi_0(r_0, \theta_0)$ is a free function that will affect the plasma velocity \mathbf{v} , and so, for a solution confined to a finite region, it represents a boundary condition on the solution. We choose here to set $\phi_0(r_0, \theta_0) \equiv 0$ since this is the condition needed for a purely counter-rotational plasma velocity that is anti-symmetric about $z = 0$. The corresponding potential, ϕ , is given as a function of r and z by

$$\phi = - \frac{\sqrt{2\pi} b_0 k L}{\sigma_0 \mu a^3} (a^2 - r^2) e^{-5r^2/a^2} \operatorname{erf}\left(\frac{\sqrt{2}z}{L}\right), \quad (15)$$

where $\operatorname{erf}(\xi)$ is the error function defined by

$$\operatorname{erf}(\xi) = \frac{2}{\sqrt{\pi}} \int_0^\xi e^{-u^2} du.$$

Thus, a jump in the electric potential across the non-ideal region exists, with the maximum potential difference being along the central field line. Outwith the non-ideal region the electric field is in the radial direction only, oppositely directed above and below central plane ($z = 0$), and confined within the flux tube consisting of field lines which thread the non-ideal region.

The component of the velocity perpendicular to the magnetic field can be deduced from (13) as

$$\mathbf{v}_\perp = \frac{(-\nabla\phi - \mathbf{j}/\sigma) \times \mathbf{B}}{|\mathbf{B}|^2}.$$

We use the freedom to add a component parallel to \mathbf{B} to ensure $\nabla \cdot \mathbf{v} = 0$:

$$\mathbf{v} = \mathbf{v}_\perp - (\mathbf{v}_\perp)_z \frac{\mathbf{B}}{b_0}.$$

The resultant velocity field is in the azimuthal direction only and given by

$$\mathbf{v} = \frac{2\eta_0 k r}{a} e^{-5r^2/a^2} \left(\frac{\sqrt{2\pi} L}{a^4} (6a^2 - 5r^2) \operatorname{erf}\left(\frac{\sqrt{2}z}{L}\right) + \frac{2z}{L^2} e^{-2z^2/L^2} \right) \hat{\boldsymbol{\theta}},$$

where $\eta_0 = 1/\sigma_0\mu$. An example is illustrated in Figure 7. The flow is counter-rotational, i.e. rotates in opposite sense above and below the $z = 0$ plane (where

it vanishes). The magnitude of the flow increases with distance from the central plane and becomes independent of height, z , in the ideal region. Non-zero flow is confined to the flux tube consisting of the field lines threading the non-ideal region.

How does this velocity compare with the order of magnitude estimate given by (5) in the previous section? Above and below the non-ideal region we may obtain an estimate of the typical plasma velocity (which, in these regions, is independent of height) by finding the maximum value of \mathbf{v} along a radial line. This maximum velocity turns out to be given by

$$v_{max} = \kappa \frac{\eta_0 k L}{a^2}, \quad (16)$$

where κ is the constant given by

$$\kappa = \left(\frac{9 + \sqrt{177}}{20} \right) \sqrt{2\pi (75 - 5\sqrt{177})} \exp\left(\frac{\sqrt{177}}{4} - \frac{15}{4} \right) \approx 5.327. \quad (17)$$

The expression (16) is in qualitative agreement with the order of magnitude estimate given by (5). We have, therefore, confirmed the intuitive estimate with the analytical model.

The motivation for our choice of η is now apparent. Since the component of the current parallel to the magnetic field is given by

$$j_{\parallel} = \frac{4b_0 k}{\mu a^3} (a^2 - r^2) \exp\left(-\frac{r^2}{a^2} - \frac{z^2}{L^2} \right),$$

there is a change in the sign of j_{\parallel} at $r = a$. A uniform resistivity would then lead to flows in each $r = \text{const.}$ plane rotating in different senses for $r < a$ and for $r > a$. Although the magnitude of the rotational flow for $r > a$ would be small, we choose to set it to zero for simplicity, by imposing a profile for η that ensures the non-ideal region is contained within the surface $r = a$. We have therefore obtained a kinematic model for the qualitative description of flux-tube disconnection outlined in Sec. II.

In this reconnection process all the field lines which thread through the non-ideal region are continually changing their connections, with each field line reconnecting to others within the same surface $r = r_0$. This is one of the features that distinguishes the 3D case from the 2D case where field lines are

cut and reconnected at a single point, and therefore the reconnection rate has a different interpretation in 3D. The field line which has the maximum difference in potential above and below the non-ideal region is identified as the reconnection line. In the present model, for symmetry reasons, the reconnection line is the z -axis. The reconnection rate is given by

$$\frac{d\Phi_{rec}}{dt} = \int \mathbf{E}_{\parallel} dl = \int \mathbf{E} \cdot \mathbf{B} ds = \int_{-\infty}^{\infty} \frac{4\eta_0 b_0 k}{a} e^{-2z^2/L^2} dz = \frac{2\sqrt{2\pi}\eta_0 b_0 k L}{a},$$

or, after substituting for v_{max} from equation (16),

$$\frac{d\Phi}{dt} = \frac{\sqrt{2\pi}}{\kappa} 2b_0 a v_{max}$$

where κ is the constant given by equation (17). Thus the reconnection rate in the kinematic model is, up to a constant factor, in agreement with the earlier qualitative estimate (6).

Previous analytical 3D reconnection models (see, for example, Ref. [29]) have taken a uniform current and localised the non-ideal region through localisation of the resistivity η alone. Such models find that the reconnection rate is independent of the parameter controlling the radius of the non-ideal region. Here we find that with a localised current this parameter, a , does become important in determining the reconnection rate.

IV Possible implications of the momentum equation

Both the order of magnitude estimate (discussed in Sec. II) and the analytical model (discussed in Sec. III) for flux-tube disconnection are kinematic analyses, i.e. they neglect the implications of the momentum equation. In this section we consider, from a qualitative perspective, the extent to which the momentum equation may effect the solutions. It was shown in Secs. II and III that there is some freedom present in the solutions presented. Specifically, the flux-tube may respond to an increase (decrease) in the magnitude of the rotational driving velocity v_0 either by an increase (decrease) in the length, l , of the non-ideal

region, or by an increase (decrease) in the number of turns present within the flux tube or by a combination of both effects. We wish to examine whether this freedom is inherent to the 3D process, or whether it arises through neglect of the momentum equation.

Assume, then, that the qualitative model presented in Sec. II also satisfies the momentum equation,

$$\rho(\mathbf{v} \cdot \nabla) \mathbf{v} = -\nabla p + \mathbf{j} \times \mathbf{B}.$$

Consider the plasma pressure along a field-line bounding the flux tube. In the central plane ($z = 0$) the plasma velocity (\mathbf{v}) vanishes and so we may estimate the pressure at the edge of the tube as

$$\begin{aligned} (-\nabla p)_{centre} + \mathbf{j} \times \mathbf{B} &= \mathbf{0} \\ \Rightarrow |-\nabla p|_{centre} &= j_z B_\theta = \frac{2k^2 b_0^2}{\mu a}. \end{aligned} \quad (18)$$

In a plane of constant z above the non-ideal region the Lorentz force vanishes and

$$\begin{aligned} (-\nabla p)_{top} &= \rho(\mathbf{v} \cdot \nabla) \mathbf{v} \\ \Rightarrow |-\nabla p|_{top} &= \frac{\rho v_0^2}{a}. \end{aligned} \quad (19)$$

Now, since the pressure must be constant along a boundary field line, the estimates for $|-\nabla p|_{centre}$ and $|-\nabla p|_{top}$ given by (18) and (19), respectively, must be equal, i.e. we have that

$$v_0 = \sqrt{\frac{2}{\mu\rho}} k b_0, \quad (20)$$

or, rewriting in terms of the azimuthal Alfvén velocity, $v_{A\theta} = k b_0 / \sqrt{2\mu\rho}$,

$$v_0 = 2v_{A\theta}.$$

We may now return to the estimate for the plasma velocity v_0 , given by equation (5), obtained in the qualitative analysis of Sec. II, i.e.

$$v_0 = \frac{2\eta k L}{a^2}.$$

Equating this last expression for v_0 with that given by (20) determines the parameter L , which determines the length of the non-ideal region, in terms of the axial field strength and flux-tube radius as

$$L = \sqrt{\frac{1}{2\rho\mu}} \frac{b_0 a^2}{\eta}. \quad (21)$$

These estimates suggest that a change in the rotational driving velocity (v_0) results in a change in the azimuthal magnetic field. The length (L) of the non-ideal region is determined by the axial field strength and tube radius. The expression for L given by (21) also allows us to estimate the ratio, L/a , between the length and diameter of the non-ideal region,

$$\frac{L}{a} = \frac{a}{\eta} v_A = R_m,$$

where v_A is the Alfvén velocity, $v_A = b_0/\sqrt{2\mu\rho}$ and $R_m = v_A a/\eta$ is the magnetic Reynolds number based on the width of the flux tube. Thus the inclusion of the momentum equation the qualitative analysis suggests that the length of the non-ideal region is very much greater than its width, resulting in a long thin current sheet.

V Conclusion

We have presented a stationary model for flux-tube disconnection. The model considers a straight magnetic flux tube which has a localised twist present in its central region as a result of a counter-rotational driving velocity imposed at the footpoints of the magnetic flux tube. The model has a non-ideal region which is localised in all three dimensions, and an electric field component parallel to the magnetic field is present within the non-ideal region. These two properties are those required for the process to be considered as an example of global general magnetic reconnection ([16]). It differs in many respects from more traditional models of 2D and 3D reconnection; the magnetic field is not of X-type structure, and the field lines are continually cut throughout the diffusion region. The model provides a further demonstration that the characteristics

of 3D reconnection are quite different to the 2D ones to which we have grown accustomed.

We expect flux-tube disconnection to be a ubiquitous process in astrophysical plasmas. For example, the solar corona is permeated by a multitude of coronal loops the ends of which are anchored in the photosphere where they are subject to photospheric motions. Spinning motions will tend to cause currents to build-up in the overlying corona, allow disconnection to occur and so for a heating of the plasma. In this paper we have presented simple qualitative and quantitative models for the disconnection process so that its physical implications, in particular the rate of reconnection, may be determined.

An order of magnitude analysis, presented in Sec. II, allows us to understand, from a qualitative point of view, how the disconnection occurs. An increase in the rotational driving velocity of the footpoints results in an increase in the number of turns present within the twisted flux tube. The number of turns may be altered by increasing the strength of the poloidal field component, increasing the length of the non-ideal region, or by a combination of both effects. A similar qualitative estimate of the reconnection rate has also been made, which was shown to be proportional to the rotational driving velocity and to the magnetic flux of the tube, i.e. the product of the magnetic field strength and the radius of the flux tube.

In Sec. III we presented an analytical incompressible model of flux tube disconnection. Just as with several such 3D reconnection models, the analysis is kinematic, in that the effects of the equation of motion have been ignored. Instead, the implications of Ohm's law and Faraday's law have been considered. The analytical solutions confirm the estimates of the flux tube geometry and strength and reconnection rate in relation to the footpoint velocity. A qualitative estimate from the equation of motion in Sec. IV implied that the ratio (L/a) of the diffusion region length to width is of order the magnetic Reynolds number. In turn this implies that normally the reconnection is slow and can only be fast when $L/H \approx R_m$.

The kinematic model offers interesting insights into the 3D reconnection pro-

cess, and in particular into how the flux-tube parameters may be determined. In future it would be useful also to include (either analytically or computationally) the equation of motion in the analysis. Such an inclusion may help to constrain some of the relations between parameters (such as L and H) that are free in this model, and would enable several other important questions to be addressed. For example, plasma acceleration is thought to be an important feature of reconnection. This is suggested by the equation of motion since regions of strong current may well also have strong Lorentz forces, as is the case in the 2D models. In turn the Lorentz forces would give rise to plasma acceleration unless they happen to be balanced exactly by the remaining forces acting on the fluid. Another argument suggesting plasma acceleration may take place is that during reconnection magnetic energy is converted to other forms, and so kinetic energy may be one of these. Thus in the future when the equation of motion is included we shall be able to determine how the plasma is accelerated in the model. Another important question regards the stability of the solution presented. For a stability analysis either knowledge of the full exact solution will be required or the problem will need to be approached numerically. A computational model of the process is therefore an important future step and may also allow questions regarding the dynamic accessibility of the solution to be addressed.

VI Acknowledgements

The authors wish to thank the MSU solar theory group for their hospitality, and both them and the UK's STFC for financial support. We also acknowledge financial support by the European Commission through the SOLAIRE network (MTRN-CT-2006-035484).

Appendix A: Solution with uniform diffusivity

In Sec. III we presented a model for flux-tube disconnection in which the magnetic diffusivity η is localised. If instead we take a uniform diffusivity η then the solutions for ϕ and \mathbf{v} are given instead by:

$$\phi = -\frac{2\sqrt{\pi}b_0kL}{\sigma_0\mu a^3} (a^2 - r^2) e^{-r^2/a^2} \operatorname{erf}\left(\frac{z}{L}\right),$$

$$\mathbf{v} = \frac{4\eta_0kr}{a} e^{-r^2/a^2} \left(\frac{\sqrt{\pi}L}{a^4} (2a^2 - r^2) \operatorname{erf}\left(\frac{z}{L}\right) + \frac{z}{L^2} e^{-z^2/L^2} \right) \hat{\boldsymbol{\theta}}.$$

The solution is seen to be similar to that given in Section III and its interpretation is still of flux-tube disconnection. In this solution the outermost section of the flux-tube undergoes a rotating motion that is of the opposite sense to that of the innermost section.

References

- [1] R.G. Giovanelli, *Nature*, 158, 81, (1946).
- [2] P.A. Sweet, In B. Lehnert, editor, *IAU Symp. 6: Electromagnetic Phenomena in Cosmical Physics*, Cambridge University Press, page 123, (1958).
- [3] E.N. Parker, *J. Geophys. Res*, 62, 509, (1957).
- [4] H.E. Petschek, *NASA Special Publication 50* (National Aeronautics and Space Administration, Washington, DC, 1964), p. 425
- [5] E.R. Priest, T.G. Forbes, *Magnetic Reconnection*. (Cambridge University Press, Cambridge, 2000).
- [6] E.R. Priest, T.G. Forbes, *J. Geophys. Res*, 91, 5579, (1986).
- [7] E.R. Priest, L.C. Lee, *J. Plasma Physics*, 44, 337, (1990).
- [8] T.G. Forbes, E.R. Priest, *Rev. Geophys.*, 25, 1583, (1987).
- [9] M. Ugai, *Computer Phys. Commun.*, 49, 185, (1988).
- [10] H. Baty, E.R. Priest, T.G. Forbes, *Phys. Plasmas*, 13, 2312, (2006).
- [11] J. Killeen, M.N. Rosenbluth, H.P. Furth, *Phys. Fluids*, 6, 459, (1963).
- [12] M. Ugai, *Phys. Plasmas*, 6, 1522, (1999).
- [13] M. Ugai, L. Zheng, *Phys. Plasmas*, 12, 2312, (2005).
- [14] M.G. Linton, D.W. Longcope, *Astrophys. J*, 642, 1177, (2006).
- [15] V. Archontis, A.W. Hood, C. Brady, *Astron. Astrophys.*, 466, 367, (2007).
- [16] K. Schindler, M. Hesse, J. Birn, *J. Geophys. Res*, 93, 5547, (1988).
- [17] W.I. Axford, *Magnetic field reconnection*, ed. E. W. Hones, Jr., (American Geophysical Union, Washington, DC, 1984) p. 1
- [18] D.W. Longcope, *Sol. Phys.*, 169, 91, (1996).
- [19] R.M. Close, C.E. Parnell, E.R. Priest *Sol. Phys.*, 225, 21 (2004)

- [20] E.R. Priest, V.S. Titov, *Phil. Trans. Roy. Soc.*, 354, 2951, (1996).
- [21] D.W. Longcope, *Phys. Plasmas*, 8, 5277, (2001).
- [22] D.I. Pontin, I.J.D. Craig, *Astrophys. J.*, 642, 568, (2006).
- [23] K. Galsgaard, Å Nordlund, *J. Geophys. Res.*, 102, 231, (1997).
- [24] C.E. Parnell, K. Galsgaard, *Astron. Astrophys.*, 428, 595 (2004)
- [25] K. Galsgaard, C.E. Parnell, *Astron. Astrophys.*, 439, 335 (2005)
- [26] A.L. Haynes, C.E. Parnell, K. Galsgaard, E.R. Priest, *Proc. Roy. Soc. A*, 463, 1097, (2007).
- [27] D.I. Pontin, G. Hornig, E.R. Priest, *Geophys. Astrophys. Fluid Dyn.*, 98, 407, may (2004).
- [28] D.I. Pontin, G. Hornig, E.R. Priest, *Geophys. Astrophys. Fluid Dyn.*, 99, 77, (2005).
- [29] G. Hornig, E.R. Priest, *Phys. Plasmas*, 10, 2712, (2003).
doi:10.1063/1.1580120.
- [30] A.L. Wilmot-Smith, G. Hornig, E.R. Priest, *Proc. Roy. Soc. A*, 462, 2877, (2006).
- [31] D.I. Pontin, K. Galsgaard, G. Hornig, E.R. Priest, *Phys. Plasmas*, 12, 2307, (2005).
- [32] I. De Moortel, K. Galsgaard, *Astron. Astrophys.*, 451, 1101, (2006).
- [33] Y-Y. Lau, J.M. Finn, *Astrophys. J.*, 366, 577, (1991).

List of Figures

1	Classification of breakdown of magnetic connection according to Ref. [16]. Various branches of General Magnetic Reconnection are shown. Reconnection is classed as <i>global</i> when a change in magnetic connectivity occurs for plasma elements that do not themselves pass through the non-ideal region.	23
2	Sketch illustrating the model for flux-tube disconnection. A flux tube of radius a is anchored at its footpoints $z = \pm H$ which are rotated in opposite directions with speed v_0 . The counter-rotation generates a localised twist within the flux tube in the shaded region, i.e. between $z = \pm L$	24
3	Sketch illustrating the form of the current generated by the counter-rotation of the flux-tube footpoints. The box indicates the boundaries of the non-ideal region. A strong current (solid black lines) gives rise to the localised non-ideal region, with the weak return current (dashed lines) being diffuse.	25
4	Path taken to consider a loop integral consisting of the central field line, a field line along the boundary of the non-ideal region (shaded) and two connecting radial lines. The integral of the electric field around the loop (solid black lines) must vanish due to the stationarity of the process. The central axis indicated by a dashed line.	26
5	Some typical field lines threading the non-ideal domain, for parameters $k = 1, a = 1, L = 3, b_0 = 1$	27
6	Vector-field illustration of the localised axisymmetric current (parameters $k = 1, a = 1, L = 1, b_0 = 1, \mu = 1$).	28
7	Counter-rotating flows (a) above ($z = 1$) and (b) below ($z = -1$) the central plane, $z = 0$. The solid line indicates the boundary 2% of the non-ideal region in the same planes (parameters $k = 1, a = 1, L = 3, b_0 = 1, \mu = 1, \eta_0 = 1$).	29

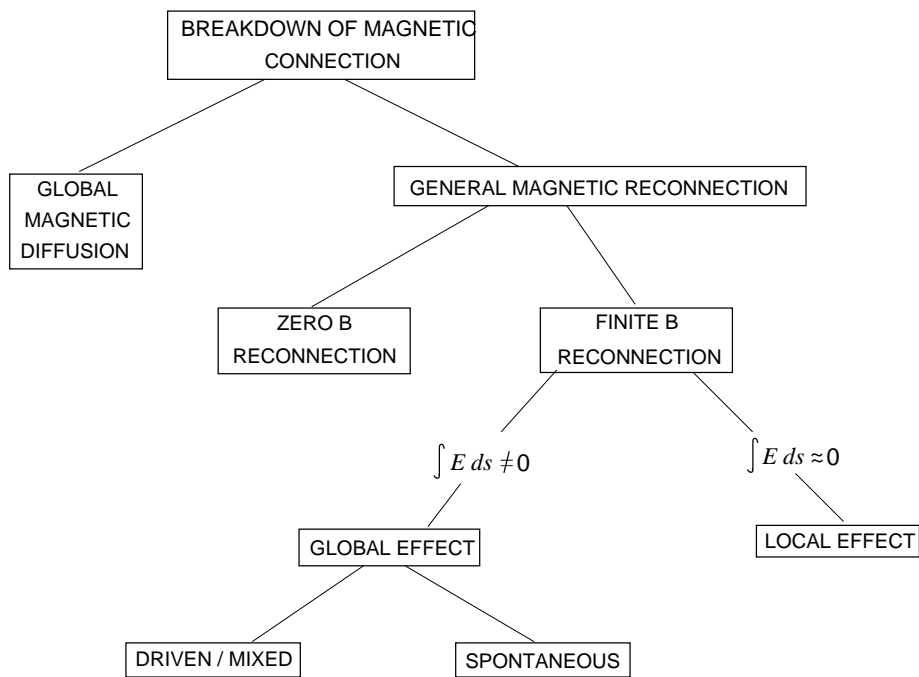


Figure 1: Classification of breakdown of magnetic connection according to Ref. [16]. Various branches of General Magnetic Reconnection are shown. Reconnection is classed as *global* when a change in magnetic connectivity occurs for plasma elements that do not themselves pass through the non-ideal region.

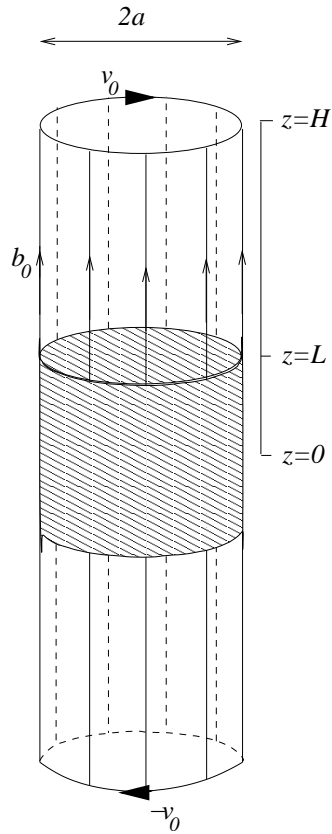


Figure 2: Sketch illustrating the model for flux-tube disconnection. A flux tube of radius a is anchored at its footpoints $z = \pm H$ which are rotated in opposite directions with speed v_0 . The counter-rotation generates a localised twist within the flux tube in the shaded region, i.e. between $z = \pm L$.

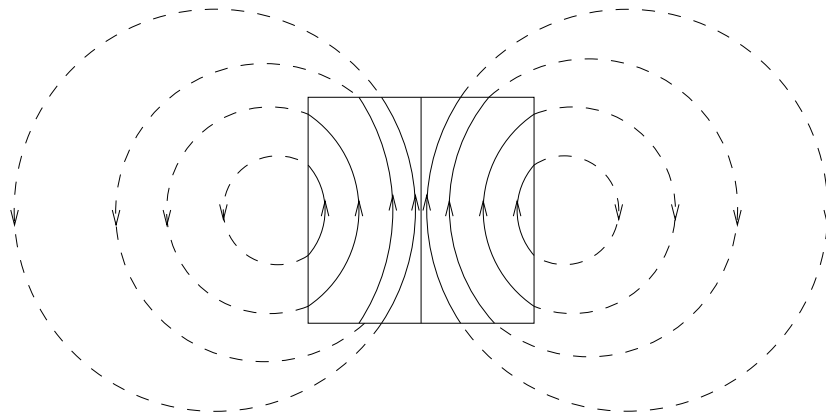


Figure 3: Sketch illustrating the form of the current generated by the counter-rotation of the flux-tube footpoints. The box indicates the boundaries of the non-ideal region. A strong current (solid black lines) gives rise to the localised non-ideal region, with the weak return current (dashed lines) being diffuse.

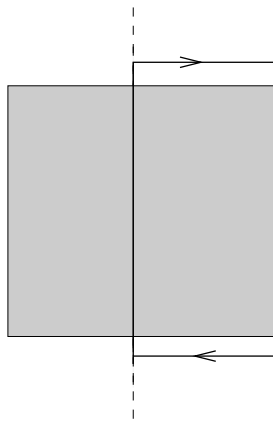


Figure 4: Path taken to consider a loop integral consisting of the central field line, a field line along the boundary of the non-ideal region (shaded) and two connecting radial lines. The integral of the electric field around the loop (solid black lines) must vanish due to the stationarity of the process. The central axis indicated by a dashed line.

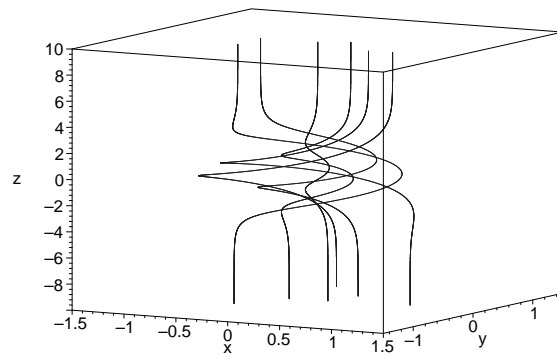


Figure 5: Some typical field lines threading the non-ideal domain, for parameters $k = 1$, $a = 1$, $L = 3$, $b_0 = 1$

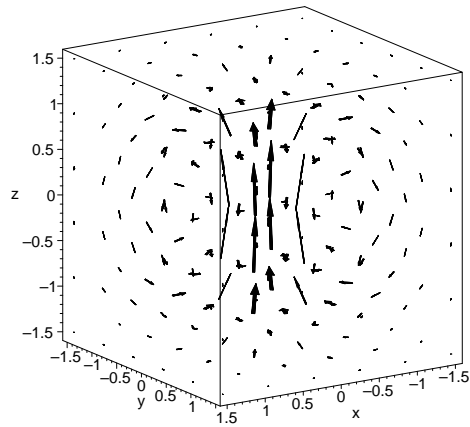


Figure 6: Vector-field illustration of the localised axisymmetric current (parameters $k = 1$, $a = 1$, $L = 1$, $b_0 = 1$, $\mu = 1$).

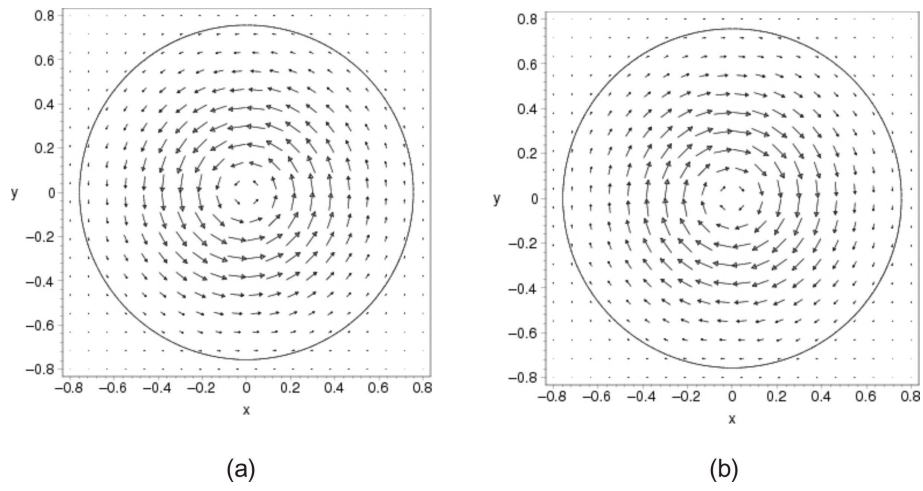


Figure 7: Counter-rotating flows (a) above ($z = 1$) and (b) below ($z = -1$) the central plane, $z = 0$. The solid line indicates the boundary 2% of the non-ideal region in the same planes (parameters $k = 1$, $a = 1$, $L = 3$, $b_0 = 1$, $\mu = 1$, $\eta_0 = 1$).